

1 **Evaluation of amorphous and lipid-based formulation strategies to increase the**
2 ***in vivo* cannabidiol bioavailability in piglets**

3 Koch N.¹, Jennotte O.¹, Bourcy Q¹., Lechanteur A.¹, Deville M.², Charlier C.², Chiap P.²,
4 Cardot J.M.³, Evrard B.¹

5 ¹University of Liège, Laboratory of Pharmaceutical Technology and Biopharmacy, Center for Interdisciplinary
6 Research on Medicines (CIRM), Liège, 4000 Belgium

7 ²Academic Hospital of Liège, Department of Toxicology, GLP-AEPT Unit, Center for Interdisciplinary Research on
8 Medicines (CIRM), Liège, 4000 Belgium

9 ³Borvo, Ceyrat, 63122 France

10 **Abstract**

11 Cannabidiol (CBD) suffers from poor oral bioavailability due to poor aqueous solubility and
12 high metabolism, and is generally administered in liquid lipid vehicles. Solid-state
13 formulations of CBD have been developed, but their ability to increase the oral bioavailability
14 has not yet been proven *in vivo*. Various approaches are investigated to increase this
15 bioavailability. This study aimed to demonstrate the enhancement of the oral bioavailability of
16 oral solid dosage forms of amorphous CBD and lipid-based CBD formulation compared to
17 crystalline CBD. Six piglets received the three formulations, in a cross-over design. CBD and
18 7 - COOH - CBD, a secondary metabolite used as an indicator of hepatic degradation, were
19 analyzed in plasma. A 10.9-fold and 6.8-fold increase in oral bioavailability was observed for
20 the amorphous and lipid formulations, respectively. However, the lipid-based formulation
21 allowed reducing the inter-variability when administered to fasted animals. An entero-hepatic
22 cycle was confirmed for amorphous formulations. Finally, this study showed that the
23 expected protective effect of lipids against hepatic degradation of the lipid-based formulation
24 did not occur, since the ratio CBD/metabolite was higher than that of the amorphous one.

25

26

27

28

29

30

31

32 **Abbreviations**

33 API = Active pharmaceutical ingredient

34 ASD = Amorphous solid dispersion

35 AUC_{last} = Area under the curve

36 BCS = Biopharmaceutics classification system

37 C_{max} = Maximum of concentration

38 CBC = Cannabichromene

39 CBD = Cannabidiol

40 CBG = Cannabigerol

41 DSC = Differential scanning calorimetry

42 EHC = Enterohepatic cycle

43 F = Absolute bioavailability

44 FaSSIF = Fasted state simulated intestinal fluid

45 GLP = Good laboratory practices

46 ICH = International Committee of Harmonisation

47 MRM = Multiple reaction monitoring

48 MS = Mesoporous silica

49 T_{max} = Time at which C_{max} is reached

50 THC = 9 Δ -tetrahydrocannabinol

51 UHPLC – MS/MS = Ultra-high pressure liquid chromatography – mass spectrometry
52 (tandem)

53 UIR = Unit impulse response

54

55 Introduction

56 Endo- and phytocannabinoids systems are nowadays widely studied since they offer new
57 possibilities of treatment. Actually, the most famous endocannabinoids, anandamide and 2-
58 arachidonoylglycerol, have demonstrated bioactivity in pathways such as neurotransmission,
59 analgesic properties, anxiolytics effects, memory information, neuroprotective effects or even
60 fertility influence (Fonseca and Rebelo, 2022). Their receptors CB₁ and CB₂ interact also with
61 phytomolecules known as phytocannabinoids. The most used phytocannabinoid is certainly
62 9Δ-tetrahydrocannabinol (THC) which is the most abundant in the *Cannabis* plant and is
63 responsible of multiple effects including drug abuse. Besides THC, a plethora of molecules
64 exists. Among them can be cited cannabidiol (CBD), cannabigerol (CBG) or
65 cannabichromene (CBC). In addition to the capacity to interact with the endocannabinoids
66 system, these molecules have antioxidant and anti-inflammatory properties thanks to their
67 chemical structure. In particular, CBD is studied since it is also abundant in *Cannabis* plants
68 and is devoid of any drug abuse risk unlike THC. This biphenolic compound is and was
69 involved in many preclinical or clinical studies. Anxiety, schizophrenia, opioids use disorder
70 or social phobia are examples of pathologies that could be treated at least partially with CBD
71 (Bergamaschi et al., 2011; Heider et al., 2022). A retrospective study has highlighted positive
72 clinical outcomes against moderate and severe symptoms of pain, anxiety and depression by
73 given orally CBD-rich products such as CBD-rich cannabis oils that contain 20 – 25 mg of
74 CBD/mL (Rapin et al., 2021). However, *Millar et al.* call for caution to all the virtues proposed
75 by many authors since almost no phase III study has shown efficacy except against epilepsy
76 (Millar et al., 2019). There are actually only two approved CBD-based medicines on the
77 market. The first one is registered as an oily solution used to reduce seizures caused by
78 Lennox-Gastaut and Dravet Syndrome (Epidiolex[®], Greenwich Bioscience, Inc). The second
79 one is a hydro-alcoholic solution that combines CBD with THC, it is used to reduce spasticity
80 induced by multiple sclerosis (Sativex[®]). The oral bioavailability of CBD is estimated at 6%
81 when solubilized in sesame oil (Millar et al., 2018; Perucca and Bialer, 2020) and could
82 explain the poor phase III success. Absence of solid dosage form could be due to low
83 aqueous solubility and low bioavailability. In addition, high inter- and intraindividual variability
84 of CBD pharmacokinetic related to its low bioavailability is highlighted (Franco et al., 2020).
85 This variability is a high drawback because plasmatic concentrations are hardly predictable
86 and inevitably impacts clinical response, since preclinical and clinical studies do not
87 personalize the doses used.

88 CBD is classified in the second category of the Biopharmaceutics Classification System
89 (BCS) as its bioavailability is limited by the aqueous solubility and dissolution rate, which is

90 pH independent. In addition, this drug suffers from a high metabolism. Therefore, CBD needs
91 challenged formulations to increase its bioavailability. Based on the physico-chemical
92 properties of the drug, different strategies and technologies are employed to present the drug
93 in its optimal form. As a lipophilic drug (LogP=6.3), CBD is often formulated with lipid
94 excipient and/or taken with fat meal. As example and widely used as reference in many *in*
95 *vitro* and *in vivo* studies, Epidiolex® contains refined sesame oil as a major solvent and
96 ethanol as a co-solvent. The tested CBD formulations are also generally liquid and are
97 presented as oil or self-emulsifying drug delivery systems (De Prá et al., 2021). This lipid
98 strategy promotes the production of endogenous surfactant that will help the *in vivo* CBD
99 solubilization. It potentiates in fact the lymphatic passage of CBD since it has been
100 demonstrated that drugs with LogP above 5 have as their preferred absorption route
101 transport via lymph (Trevaskis et al., 2008; Yáñez et al., 2011). This pathway is also the
102 preferred route as fatty acids are present in intestinal cells. The formation of chylomicrons
103 can thus transport lipophilic drugs directly into the systemic circulation via the lymph without
104 passing through the liver. The liquid-lipid formulations have also some drawbacks
105 considering the processability, the manufacturing, the stability and the patient compliance.
106 Lipids are prone to oxidation reactions and the liquid state favors the instability of CBD.
107 Some lipid components, such as sesame oil, have allergenic properties like many seed oils
108 (Feeney et al., 2016). Besides the lipid strategy, many other formulations have been
109 investigated. Although being a grease ball molecule, the use of the amorphous form of CBD
110 prone to a high enhancement of CBD solubility and dissolution rate *in vitro*. As examples,
111 amorphous solid dispersions (ASD) of CBD have been successfully developed as well as
112 CBD-cyclodextrins complexes and mesoporous loaded silica (Jennotte et al., 2022; Koch et
113 al., 2020). The mesoporous silica formulations allow obtaining free flowing powders of
114 amorphous drugs thanks to high surface area of the inorganic carrier. If the adequate pore
115 size and loading method are chosen, stable mesoporous materials with high degree of drug
116 loading can be achieved (Koch et al., 2022). *In vivo* performances of mesoporous
117 formulations have already been demonstrated for some BCS II drugs such as fenofibrate,
118 celecoxib, asarone or itraconazole (Bukara et al., 2016; Mellaerts et al., 2008; Riikonen et al.,
119 2015; Zhang et al., 2015).

120 The aims of this work were therefore to study for the first time the *per os* bioavailability of
121 CBD in piglets in solid state within three different formulations: an amorphous formulation of
122 CBD, a lipid-based CBD formulation and a crystalline CBD powder. Piglets were selected
123 because they have a digestive tract similar to that of humans, including a gall bladder.
124 Moreover, the hepatic metabolization of CBD within the formulation was evaluated by

125 following the concentration of the metabolite 7 – COOH – CBD, indicating potential protective
126 effect from the first pass metabolism.

127

128 **EXPERIMENTAL METHODS**

129 **Materials**

130 CBD was purchased from THC Pharm (Germany); mesoporous silicas (MS) Syloid[®] XDP
131 3050 and Silsol[®] were kindly donated by W.R. Grace (Germany), Gelucire[®] 50/13 was kindly
132 gifted by Gattefossé (France). FaSSIF powder was purchased from Biorelevant[®] (United
133 Kingdom). Hydrochloric acid (HCl 37%) and sodium hydroxide were purchased from Merck[®]
134 (Germany). CO₂ (99.998%) was supplied by Air Liquide (Liège, Belgium). Deuterium-CBD, 7
135 – COOH – CBD and deuterium 7 – COOH – CBD were purchased from Sigma Aldrich.
136 Acetonitrile was HPLC grade, and methanol, water, ethyl acetate and n-hexane were UHPLC
137 grade.

138 **Production of CBD formulations**

139 *Amorphous formulation*

140 Amorphous formulation used in this study has been developed and published by the current
141 team (Koch et al., 2020). Further information such as the influence of the pore size could be
142 found in the concerned publication. It consists of mesoporous silica Silsol (pore size: 6.6 nm)
143 impregnated by CBD (60:40) in subcritical CO₂ conditions. A high-pressure cell (TOP
144 Industrie, France) was filled with appropriate mass of Silsol MS and CBD. After closed, the
145 cell was immersed in a water bath set at 50 °C and filled with CO₂ at the pressure of 60 bars,
146 with a magnetic stirring set at 200 rpm. The system was finally depressurized after one hour.
147 Final formulation was manually conditioned in 00 sized gelatin capsules without further
148 formulation.

149 *Lipid-based formulation*

150 Lipid-based formulation was also developed by the current team (Koch et al., 2023). It
151 consists of mixture of CBD and Gelucire[®] 50/13 incorporated in Syloid MS (pore size: 25 nm)
152 in proportions 20:40:40 (CBD:Gelucire:XDP). CBD and Gelucire were melted in a water bath
153 set at 70 °C. Once both components melted and homogeneously mixed, MS XDP was
154 manually added in order to obtain a free flowing powder. Final formulation was manually
155 conditioned in 00 sized gelatin capsules.

156 *Crystalline formulation*

157 Prior to conditioning in gelatin capsules, crystalline CBD powder was sieved through a 0.4
158 mm mesh sieve to avoid any agglomerate.

159 **CBD formulations characterization:**

160 *Content and homogeneity*

161 CBD content in each formulation has been determined in triplicate by using a HPLC-UV
162 validated method (Koch et al., 2020). Zorbax[®] C18 300 SB analytical column with particles of
163 3,5µm (150 mm × 4.6 mm ID) was used with a mobile phase composed of a mixture of water
164 and acetonitrile (38/62% v/v). The flow rate was set at 1.0 mL/min, the column temperature
165 was kept constant at 30 °C and the detection wavelength was 240 nm. Formulations were
166 dissolved in acetonitrile prior to sonication. Sonicated suspension were then filtered through
167 0.45 µm PTFE filter and analyzed.

168 *Differential scanning calorimetry (DSC)*

169 Approximately 10 mg of powder was weighted, crimped in an aluminum pan and then
170 subjected to one heating ramp at a rate of 20 °K/min ranging from 25 °C to 100 °C to be
171 within the range of CBD's melting point (68 °C). The equipment used for this study was a
172 Mettler-Toledo[®] DSC 1 (Schwerzenbach, Swiss) controlled by the STARe System software.

173 *Concentration at saturation of CBD in FaSSIF medium*

174 The concentration at saturation of raw CBD in FaSSIF (fasted stated simulated intestinal
175 fluid) has been determined by adding excess of CBD in media placed in a water bath set at
176 37 °C and a rotating speed of 100 rpm during 24 hours (triplicate). After this time, the
177 suspension was filtered through PTFE 0.45 µm filter and diluted prior to HPLC analysis.
178 FaSSIF medium was prepared as recommended by Biorelevant[®] (London, UK).

179 *In vitro dissolution test*

180 The *in vitro* dissolution performance of crystalline CBD and both amorphous and lipid-based
181 formulations were tested and compared in simulated intestinal fluid FaSSIF (Biorelevant[®],
182 London, UK) media under sink conditions. FaSSIF has been chosen considering
183 bioavailability studies performed with pig species (McCarthy et al., 2017; O'Shea et al., 2017;
184 Perlstein et al., 2014). Dissolution tests were performed by using USP II paddle method
185 (Sotax AT7, Suisse). For each formulation, equivalent of 10 mg of CBD in 00 sized gelatin

186 capsules were immersed in 500 mL of medium set at 37 °C. Dissolution tests have been
187 done during 4 hours (withdrawals at 5, 15, 30, 45, 60, 90, 120, 180 and 240 minutes) in
188 triplicate with a paddle speed set at 100 rpm. Every withdrawal was filtered through 0.45 µm
189 PTFE filter prior to HPLC-UV dosage. Means and standard deviations of *in vitro* data were
190 calculated using GraphPad Prism 5.0 software.

191 ***In vivo* study**

192 *In vivo* study was performed within PigForLife® (CER Group Facilities) GLP structure
193 (Marloie, Belgium). The study protocols were approved by the Local Ethical Committee
194 before the start of the study and complied with the Belgian regulation as published in «Royal
195 Decree of May 29, 2013 on the protection of experimental animals, A.G.W. 30.11.2017».

196 *Per os* study was conducted by given orally an equivalent of 2.5 mg CBD/kg in fasted state.
197 This dosage was selected based on Epidiolex® posology and dosage form volume. The
198 amorphous and lipid-based formulations were compared to the crystalline CBD. All
199 formulations were sealed manually in gelatin 00 sized capsules without any additional
200 excipient and administered by force-feeding system. Six Large White piglets (male and
201 female, between 8 and 20 kg) born on site and in a healthy condition were used. Due to the
202 exploratory nature of the study, a number of six was chosen arbitrary. The animals were
203 housed together in pens of about 40m² and enriched environment was provided. Natural
204 temperature and light cycle were used in a straw litter. During storage, animals were *ad*
205 *libitum* fed with pellet food balanced without any curative or preventive veterinary medicinal
206 products or veterinary additives. Tap water was available *ad libitum* during the entire study
207 period, including accommodation and sampling days. Piglets were fasted overnight (food but
208 not water) before giving the formulations and were then fed 6h and 12h post-dose to avoid
209 hypoglycemia. All piglets were clinically examined before the study and before sampling.
210 Each piglet received the three formulations in a randomized order with a wash-out period of
211 one week (Table 1).

212 Blood sampling (5 mL) were done in EDTA tube at time zero, 1h, 2h, 2.5h, 3h, 3.5h, 4h, 4.5h,
213 5h, 5.5h, 6h, 7h, 8h, 12h and 24h. The samples were stored at 4°C and then centrifuged at
214 2500g for 10 minutes. Plasma samples were separated from the figurative elements of blood
215 and were frozen at -80°C until their dosage.

216

217

218

Table 1 - Randomization of the *per os* study

Piglet	Week 1	Week 2	Week 3	Week 4
P1	Amorphous	Lipid-based	x	Crystalline
P2	Crystalline	Amorphous	Lipid-based	x
P3	x	Crystalline	Amorphous	Lipid-based
P4	Lipid-based	x	Crystalline	Amorphous
P5	Amorphous	Lipid-based	x	Crystalline
P6	Crystalline	Amorphous	Lipid-based	x

219

220 *Bioanalysis*

221 CBD and 7 – COOH – CBD were simultaneously quantified by a validated UHPLC – MS/MS
 222 method based on ICH M10 guidelines (Koch et al., 2024). Briefly, 500µL of plasma samples
 223 were fortified with 20 µL of internal standards solution (250 ng/mL of cannabidiol-d₃ and 2000
 224 ng/mL of 7 – COOH – CBD –d₃), 100 µL of 10% anhydrous glacial acetic acid and analytes
 225 were extracted with 5mL of n-hexane/ethyl acetate (9/1 v/v) by stirring and centrifugation
 226 processes. The supernatant was transferred into vials prior to drying. Once dried, 100 µL of
 227 methanol/water (50/50) was added to dissolve the residue and transferred to Eppendorf vials
 228 prior to centrifugation and UHPLC vial filling. Samples were analyzed with a Water Xevo™
 229 TQ-S mass spectrometer interfaced with a Waters Acquity® UPLC I-Class inlet system. An
 230 Acquity® UPLC BEH C18 (1.7µm (2.1 x 50 mm)) column set at 45°C was used as stationary
 231 phase and the mobile phase consisted in a mixture of ammonium bicarbonate buffer (pH10)
 232 and methanol in a gradient mode, with a flow rate of 0.45mL/min. Injection volume was 1µL
 233 for a run time of 6 minutes. Positive electrospray ionization mode was used and two MRM
 234 transitions (m/z) were used for identification and quantification of CBD and 7 – COOH –
 235 CBD. Calibration curves and QC were daily prepared and data acquisition was achieved
 236 using MassLynx Version 4.2 software and TargetLynx Version 4.2 software.

237 *Pharmacokinetic analysis*

238 Concentrations versus time *in vivo* data and pharmacokinetic parameters C_{max} , T_{max} and
 239 AUC_{last} were analyzed by a non-compartmental pharmacokinetic analysis using Phoenix™
 240 WinNonlin 8.4 (Certara, Princeton, USA). Linear trapezoidal linear interpolation calculation
 241 method was applied for AUC_{last} , C_{max} correspond to the highest concentration observed and
 242 T_{max} is the time requested to achieve C_{max} . Deconvolution process has been performed by

243 using unit impulse response (UIR) from intravenous data in piglet provided by the current
244 team and published elsewhere in order to construct the input rate and fraction absorption
245 graphs (Koch et al., 2024). All measured concentrations (C) were normalized with the
246 administered dose. If the concentration at T₀ (C₀) differed from 0 ng/mL, correction was made
247 by using the following formula (Eq.1):

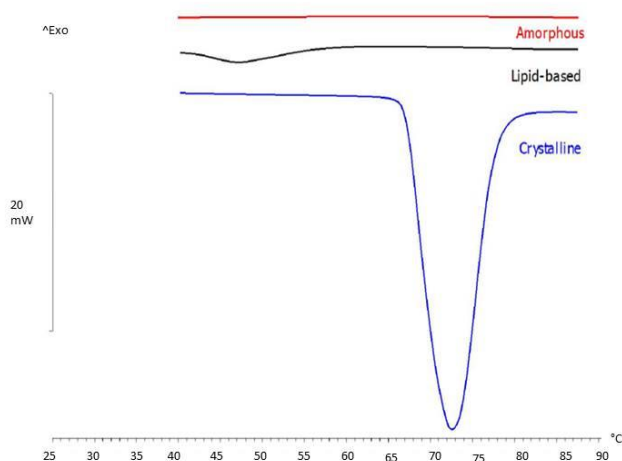
248
$$\text{Corrected concentration (If } C_0 \neq 0 \text{ ng/mL)} = C - (C_0)^{t*0.34} \quad (\text{Eq. 1})$$

249 Where C₀ is the concentration observed at time 0h, t the time of sampling, 0.34 is the overall
250 terminal elimination obtained after intravenous administration (Koch et al., 2024). Phoenix™
251 WinNonlin 8.4 software was used to calculate the means and standard deviations of *in vivo*
252 data.

253 Results and discussion

254 CBD content and physical state

255 Results on drug content analysis by HPLC revealed that CBD content in all used
256 formulations of this study was between 95 and 105%, suggesting that formulation process
257 induced no significant drug degradation or loss. Additionally, amorphization of CBD within the
258 amorphous and lipid-based formulations was confirmed by DSC prior to *in vitro* dissolution
259 and *in vivo* study as shown on Figure 1. The formulations were therefore stable for all the
260 duration of the current *in vitro* and *in vivo* experiments.



261

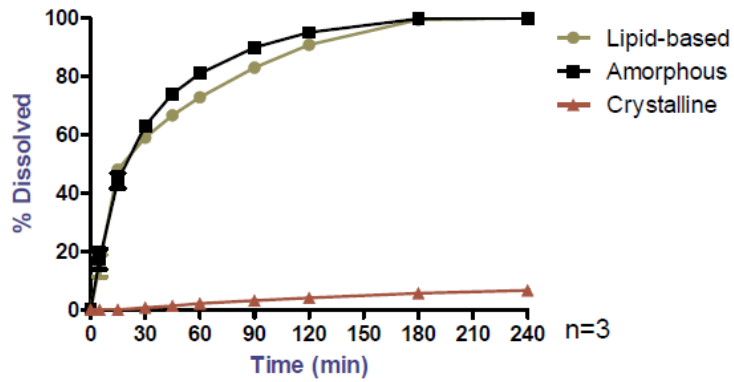
262

Figure 1 – Thermograms of amorphous and lipid-based formulations, compared to the crystalline CBD

263 Both lipid-based and amorphous formulations presented a non-crystalline state of CBD.
264 Amorphous formulation is a purely non organized state of CBD stabilized inside mesoporous
265 network while the lipid-based formulation is a solid solution of CBD within the lipid material.
266 The release of CBD from the amorphous formulation is inherent of its interaction with the
267 silica surface. On the other side, the lipid-based formulation presents CBD in a fine
268 interaction with lipids contained in the formulation. The release of CBD outside the silica is
269 therefore dependent on a preliminary step of solubilizing the CBD-Gelucire[®] 50/13 mixture
270 inside the mesopores, which must then exit the silica pores by diffusion.

271 ***In vitro* dissolution test**

272 FaSSIF medium simulates the fasted intestinal fluid with a pH of 6.5 and contained 3 mM of
273 taurocholate and 0.75 mM of phospholipids, namely lecithin. This media mimics the intestinal
274 fluids in terms of pH, isotonicity and surfactant characteristics, under fasted conditions
275 (Henze et al., 2019). The concentration at saturation of crystalline CBD in FaSSIF medium
276 has been determined at 62.17 ± 2.70 $\mu\text{g/mL}$. As the actual water solubility of CBD is given in
277 the literature at 0.39 $\mu\text{g/mL}$ (Grifoni et al., 2022), this result shows the importance of the
278 presence of surfactants and/or phospholipids to increase the CBD solubility. Since CBD is a
279 BCS II molecule, its bioavailability is theoretically limited by the solubilization. Sink conditions
280 were thus chosen since it is expected that all drug dissolved will readily be absorbed. The
281 dissolution should therefore be little or not influenced by what has already been dissolved.
282 Equivalent of 10 mg were tested. The dissolution rate of the crystalline CBD was very slow
283 and only $6.72 \pm 0.86\%$ of CBD was dissolved after four hours. The release profile of the
284 crystalline form was not studied further, as its kinetic was too slow compared with the other
285 two formulations. With the two other formulations, dissolution tests showed a rapid but no
286 immediate release of CBD since 80% are dissolved after 60 min and 90 min for the
287 amorphous and the lipid-based formulation respectively (Figure 2). This could be explained
288 by the more complex solubilization process of the lipid-based formulation discussed further.
289 Formulating CBD as pure amorphous state or in mixture with lipid allow a complete release
290 *in vitro* of the drug after 180 min.



291

292

Figure 2 – *In vitro* dissolution tests of crystalline, amorphous and lipid-based formulations in FaSSIF medium (n=3; ± SD)

293

294

The dissolution data were fitted to Weibull equation model (Eq. 2; Figure 3).

295

$$F_{inf} * \left(1 - e^{\left(\frac{t}{MDT}\right)^B}\right) = \% \text{ dissolved} \quad (\text{Eq.2})$$

296

Where F_{inf} is the maximum of dissolution (i.e. 100% if dissolution is complete), t the time,

297

MDT the mean dissolution time and b the slope factor. Amorphous and lipid-based

298

formulations have a Weibull kinetics release profile under sink conditions in FaSSIF media as

299

evidenced by correlation coefficients of 0.999 and 0.997 respectively.

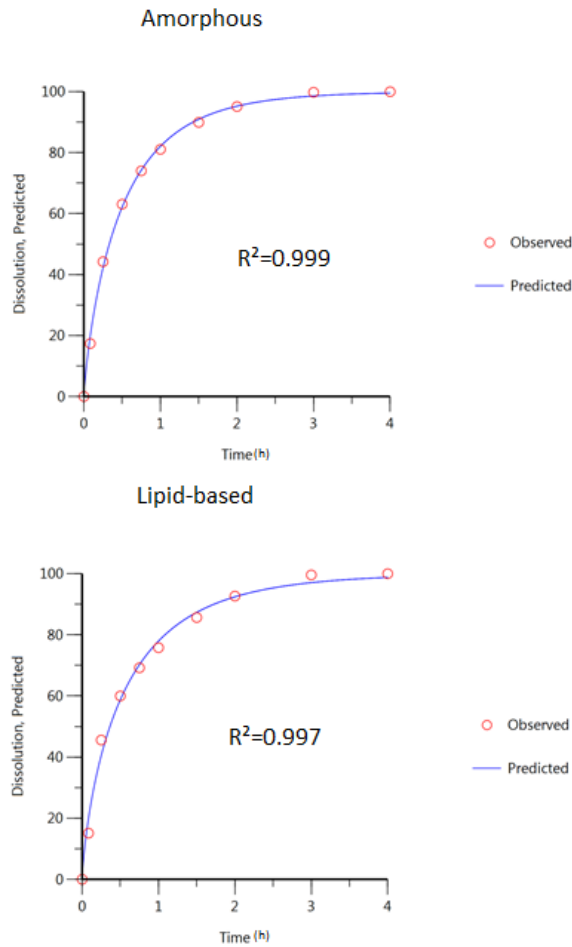


Figure 3 – Observed and Weibull based predicted values plots

300
301

302 The b exponent, determined at 0.82 and 0.77 for the amorphous and lipid-based formulation
 303 respectively, characterizes the mechanism of exponential drug release. When the b value is
 304 situated between 0.75 and 1, the release mechanisms are a combination of diffusion and
 305 another effect (Papadopoulou et al., 2006). As example, Corsaro et al. described a
 306 combination of Fickian diffusion and swelling controlled transport (Corsaro et al., 2021). If
 307 swelling effect could occur with the lipid-based formulation, the amorphous one is not
 308 susceptible to it. The fit considering the Korsmeyer-Peppas equation (Eq.3) give n-values
 309 below 0.43 for both formulation, which also indicates a predominant Fickian diffusion (Table
 310 2) (Tomic et al., 2018).

311

$$\% \text{ dissolved} = K * t^n = \frac{Mt}{M_{\infty}} \quad (\text{Eq. 3})$$

312 Where K is the release rate constant, n is the release exponent, Mt/M_{∞} is the drug release at
 313 time t.

314 While both formulations initially showed a CBD release related to the gradient concentration,
315 the amorphous formulation sees its release slow down over time probably due to the need
316 for fluids to go deeper into the pores of mesoporous silica, and the lipid-based formulation
317 sees the addition to the two precedent release mechanism of a lipid digestion process.

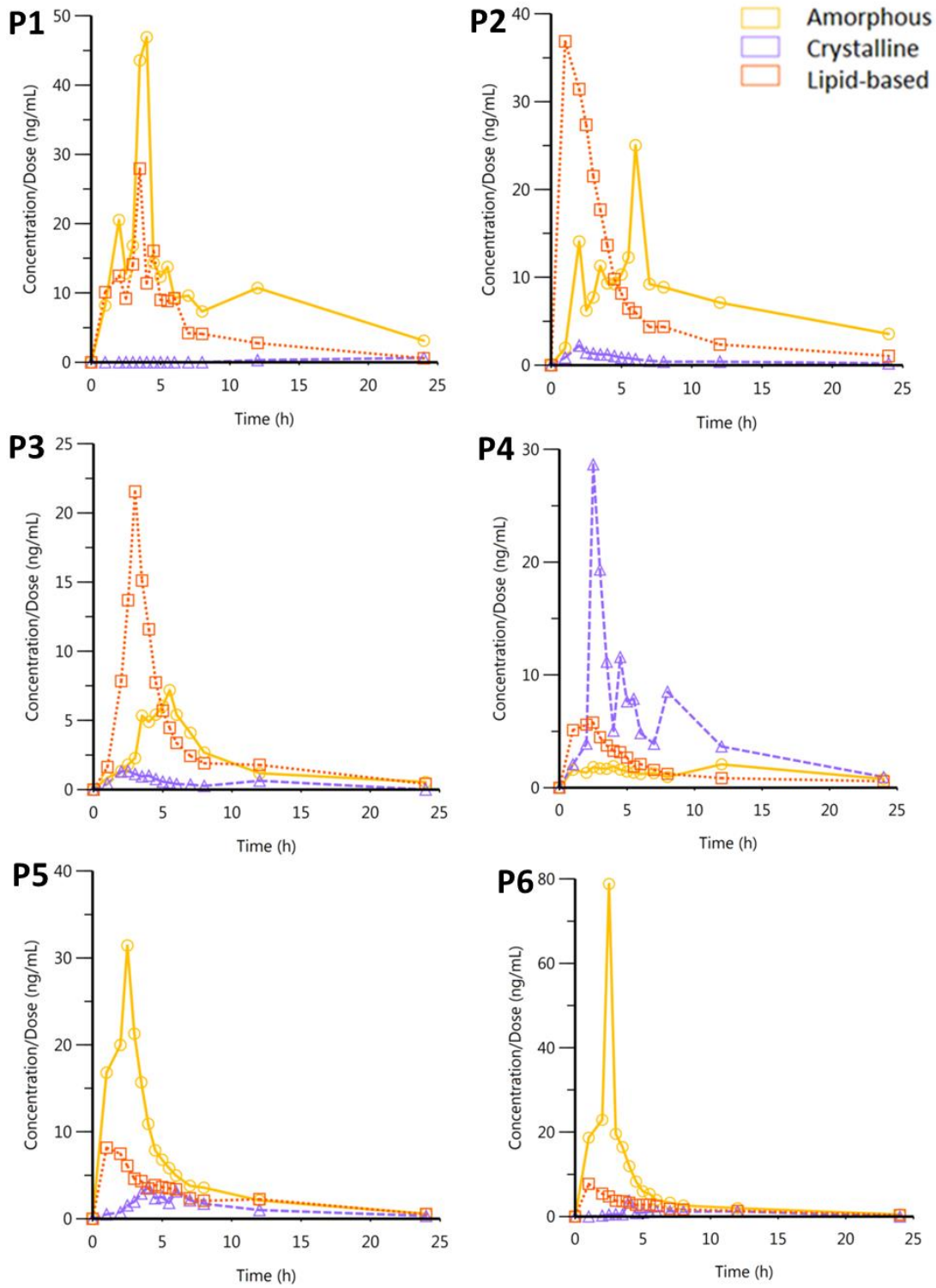
318 **Table 2 - Korsmeyer - Peppas equation parameters**

Fitting	K	n	r ²
Lipid-based	19.19	0.32	0.977
Amorphous	21.27	0.30	0.971

319

320 ***In vivo* study**

321 All animals were daily checked during the study and evident signs of toxicity, general
322 appearance, viability, mobility and stools were examined and no abnormality was detected.
323 The wash-out period used in this study (one week) was adequate since almost all T₀ were
324 quantified at 0 ng/mL, except for two single time points. Among the six piglets, one non-
325 concordant animal was detected. Indeed, the bioavailability of crystalline CBD in one specific
326 piglet (P4) was much higher than the two formulations and that were completely different
327 from the results obtained with the five others piglets (Figure 4). P4 was in fact the one
328 concerned by the presence of the two time point concentrations at T₀ which differed from 0
329 ng/mL. To take into account this afterglow, the concerned plasmatic concentration values
330 were corrected as detailed above (Eq. 1). For P1, P2, P3, P5 and P6, amorphous and lipid-
331 based formulations allow a significant enhancement of bioavailability of CBD in comparison
332 with the crystalline CBD. Moreover, the individual concentration vs time curves show a high
333 variability between the animals. It is observed that the amorphous and lipid-based curves
334 never show similar exponential phases from T₀ to T_{max} for a same piglet. Pharmacokinetic
335 parameters T_{max}, C_{max}, and AUC_{last} calculated from the data using the six piglets showed
336 higher variability for the amorphous formulation in comparison with the lipid-based
337 formulation (Table S1, Supplementary materials). This may be due to the fact that the
338 formulations require different digestive process and metabolism pathway to *in fine* allow the
339 CBD release and absorption. The genetic variability provides piglets with different metabolic
340 and digestive capacity (Noblet et al., 2013). As access to water was not controlled, some
341 piglets could have drink more and have accelerated transit with for example less contact with
342 gastric medium or diluted gastric fluid with higher pH. These factors may have influenced the
343 CBD absorption from the two optimized formulations and from crystalline materials, leading
344 partially to the observed intervariability.



345

346

347

Figure 4 – Individual time vs concentration curves of CBD (2.5 mg/kg) for the three formulations (Amorphous, lipid-based and crystalline). Please note that the scale is different in function of the piglet.

348 As the fourth piglet (P4) showed a completely different behavior and showed a high AUC and
 349 C_{max} for the crystalline form of CBD, it was decided to exclude this piglet from the main
 350 analysis since it modified considerably the results and biased the bioavailability assessment.

351 Attention has to be made on the fact that the results directly depend on the variability. In
 352 particular, T_{max} values are highly influenced by the presence of at least two peaks for the
 353 amorphous formulation while the crystalline and lipid-based formulations have mostly one
 354 single peak. T_{max} is indeed associated with the C_{max} and not always with the first peak. This
 355 problematic has been widely reviewed and authors discussed the fact that choosing to work
 356 with mean or individual curves may considerably influence the interpretation of the results
 357 (Cardot and Davit, 2012). In this work, we choose to provide first individual-curves-related
 358 values and secondly to use the mean curves. While the AUC_{last} of crystalline CBD reached
 359 $13.25 \pm 8.82 \text{ ng}\cdot\text{h}\cdot\text{mL}^{-1}$, amorphous and lipid-based formulations reached respectively
 360 144.47 ± 72.55 and $89.97 \pm 46.00 \text{ ng}\cdot\text{h}\cdot\text{mL}^{-1}$ (Table 3). This is an increase in relative
 361 bioavailability of 10.90 and 6.79 fold for the amorphous and lipid-based formulation. T_{max} was
 362 reached after about 4.1 ± 1.64 hours for the amorphous formulation ($C_{max} = 37.87 \pm 26.95$
 363 ng/mL), 1.9 ± 1.24 hours lipid-based formulation ($C_{max} = 20.44 \pm 12.65 \text{ ng/mL}$) and 7.3 ± 9.38
 364 hours for crystalline CBD ($C_{max} = 2.31 \pm 1.37 \text{ ng/mL}$). For amorphous formulation, a first peak
 365 is observed, close to that observed for lipid-based formulation. However, this peak is not
 366 always correlated with the highest concentration and is therefore not calculated as a T_{max} but
 367 must be taken into account when studying the speed at which CBD appears in the blood.
 368 Indeed, the first peak provided by the amorphous formulation appears at similar time than
 369 T_{max} of lipid-based formulation. This could be correlated with the similar *in vitro* dissolution
 370 rate of both formulations.

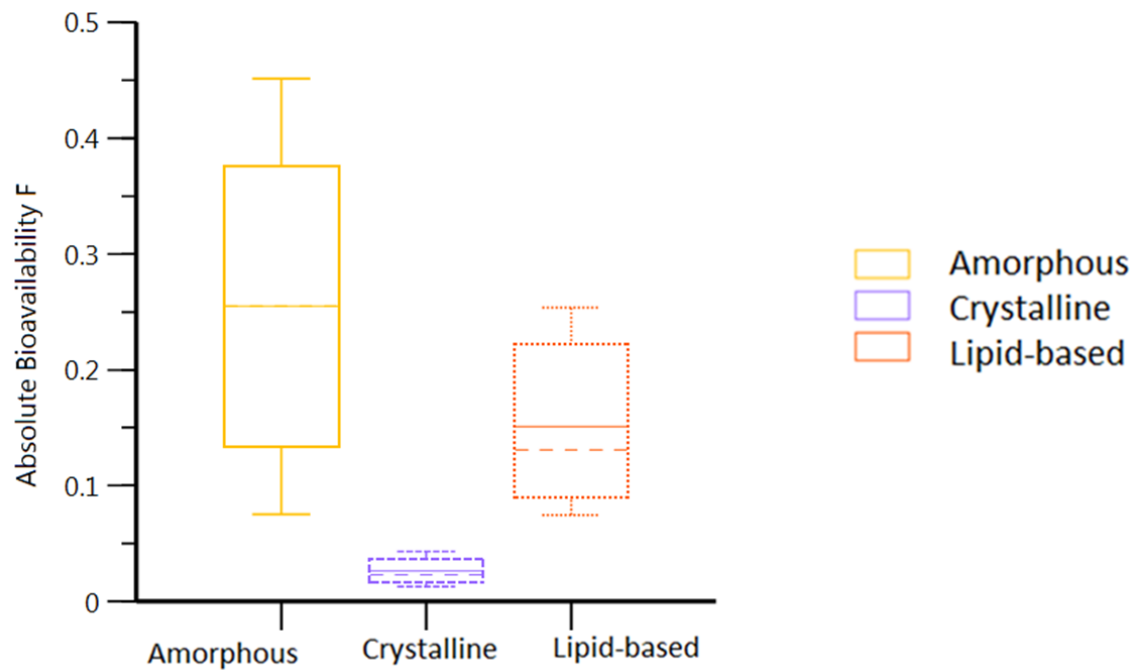
371 **Table 3 – Mean (\pm SD) of pharmacokinetic parameters obtained from individual curves (CBD dose 2.5 mg/kg; n=5)**

	Amorphous	Lipid-based	Crystalline
$AUC_{last} \text{ (ng}\cdot\text{h}\cdot\text{mL}^{-1})$	144.47 ± 72.55	89.97 ± 46.00	13.25 ± 8.82
$C_{max} \text{ (ng/mL)}$	37.87 ± 26.95	20.44 ± 12.65	2.31 ± 1.37
$T_{max} \text{ (h)}$	4.1 ± 1.6	1.9 ± 1.2	7.3 ± 9.4

372 Amorphous formulation presented virtually a high quantity of isolate molecules of CBD that
 373 are directly prone to be solubilized and absorbed. Indeed, DSC results suggest a complete
 374 amorphization of the material and a monolayer loading is approached. Once absorbed, the
 375 amorphous CBD-loaded silica particles release the CBD rapidly and with high intensity
 376 because no other release mechanism occurs than Fickian diffusion. Besides, the lipid-based
 377 formulation must follow several steps before presenting the CBD in solubilized state in the
 378 intestinal tract. These differences may lead to the higher AUC_{last} and higher C_{max} observed

379 with the amorphous formulation in comparison with the lipid-based formulation. Interestingly,
380 these results are in accordance with the work of *Bukara et al.* who compared the
381 enhancement of fenofibrate bioavailability from an ordered mesoporous formulation and from
382 the commercial lipid product Lipanthyl[®] in humans. Equally to the results presented in our
383 study, their amorphous formulation provided a higher C_{max} normalized per dose and higher
384 AUC_{last} in comparison to the lipid-based formulation (Bukara et al., 2016). Fenofibrate is
385 actually a grease ball BCS II molecule used to treat hyperlipidemia with similar LogP and
386 melting point as CBD. Our hypothesis is that the absorption of CBD from the amorphous
387 formulation depends on the quantity of digestive fluid (that contains endogenous surfactants)
388 present at the moment of absorption, whereas this is less the case for the lipid-based
389 formulation. Given that some piglets are likely to have high capacity to absorb CBD from the
390 amorphous formulation into the bloodstream, some C_{max} are high and increase the mean
391 value. The amorphous formulation therefore requires the presence of physiological elements
392 enabling absorption. The lipid formulation seems more complicated to absorb, but more
393 homogeneous between piglets, which is explained by the presence of self-emulsifying lipids
394 in the formulation, enabling equivalent digestion in all piglets, whatever their digestive
395 capacity.

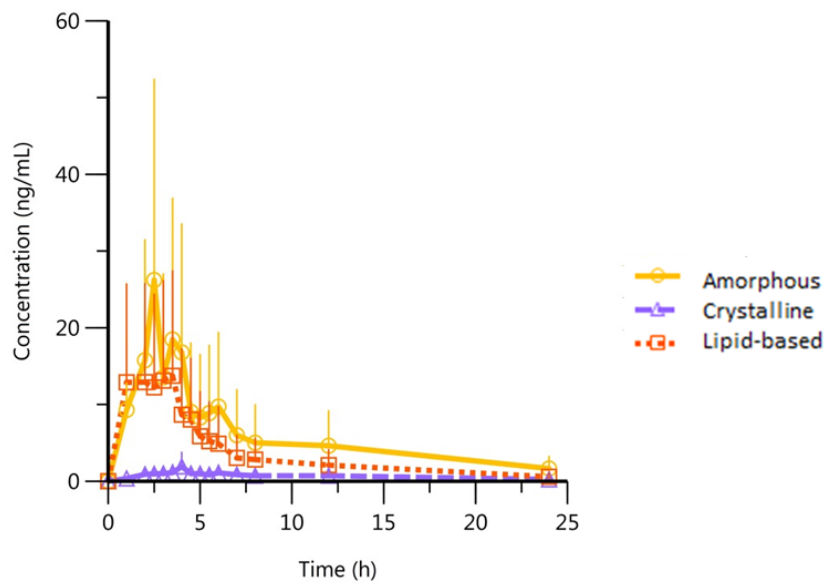
396 Deconvolution process by using UIR from a two compartment model provided by data
397 obtained with an intravenous pharmacokinetic study in piglet (Koch et al., 2024) allowed
398 constructing the CBD absorption profile from the three tested formulations. Absolute
399 bioavailability (F) obtained from the five piglets is shown on Figure 5. Although the
400 amorphous formulation achieved the highest absorption, it also suffered from high variability,
401 unlike the lipid-based formulation. As the formulations were given to fasted piglets, the self-
402 emulsification properties of the Gelucire[®] 50/13 reduced the inter-variability since every piglet
403 started equally the study as they received an adequate and identical quantity of surfactant
404 via the formulation. It is clear that both formulations allowed a high enhancement of CBD
405 absorption in comparison with the pure and crystalline form thanks to an increase
406 solubilization capacity.



407
408

Figure 5 – Bioavailability of CBD depending on the formulation (n=5)

409 The mean curves showed an apparent enterohepatic cycle (EHC), mainly for amorphous
 410 formulation, as shown on Fig 6. Indeed, the multiple peaks observed with the amorphous
 411 formulation reflect the individual curves and be possible EHC. For the lipid-based
 412 formulation, the observed plateau is less reflecting individual curves.



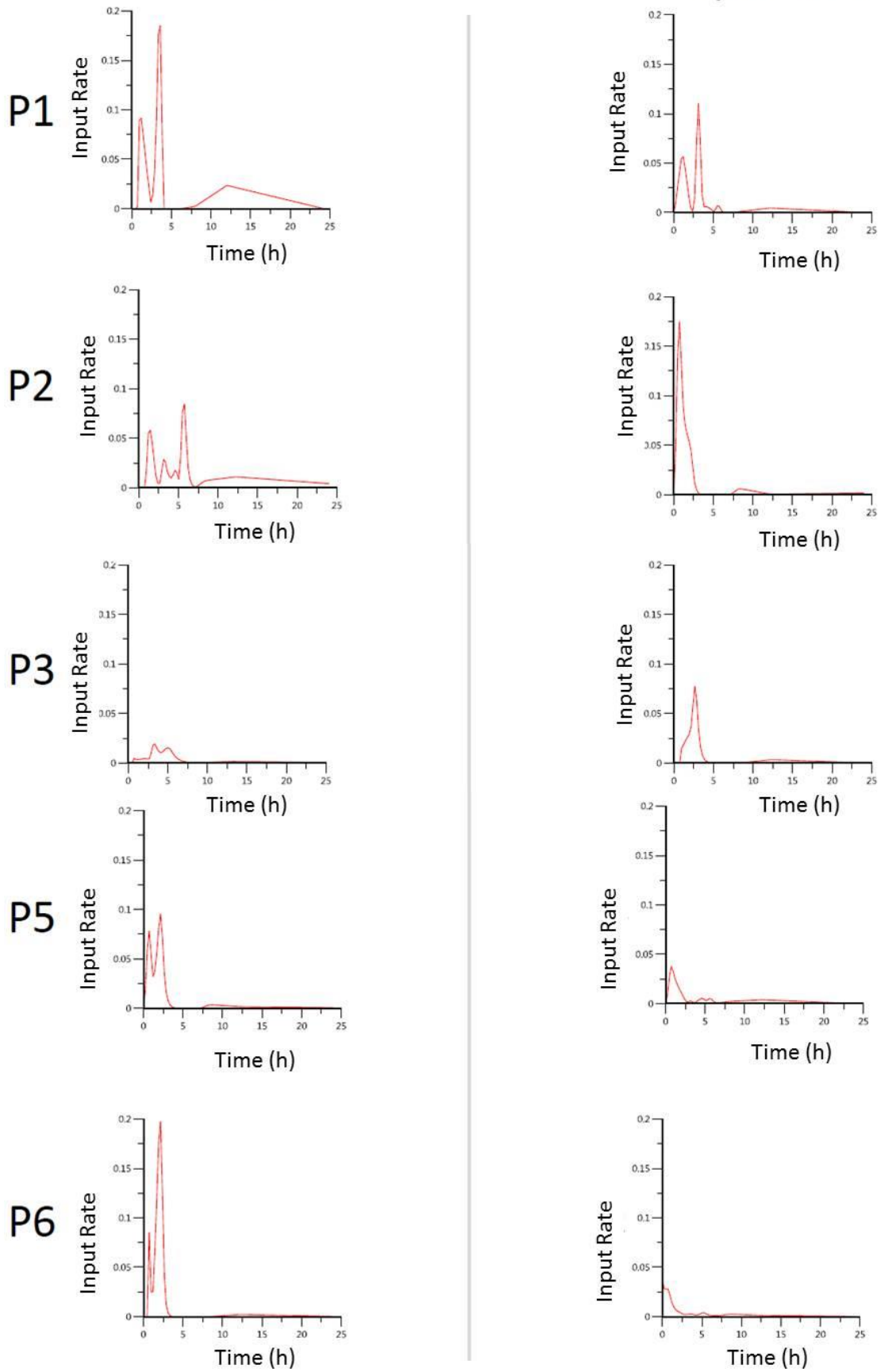
413
414

Figure 6 - Mean curves (\pm SD) of CBD concentration following administration of 2.5 mg/kg (n=5)

415 As a reminder, EHC occurs when either a glucuroconjugated metabolite formed in the liver -
416 or untransformed drug - passes through the gallbladder and is released in the intestinal tract
417 with bile. In contact with digestive enzymes, the glucuroconjugate may revert to its original
418 form and be reabsorbed; resulting in a second, or even third, peak often linked with time of
419 meals. This effect leads to a longer contact of the body with the drug and increases thus the
420 AUC_{last} . The question arises as to whether the apparent EHC observed on the mean curves
421 is due to a real reabsorption of product release by the bile or whether this EHC form-like is
422 due to a large variability in terms of T_{max} depending on the individual. Again, the problem of
423 using the individual or the mean curves is highlighted. If the figure 4 showed two peaks when
424 amorphous formulation was administrated, the lipid-based formulation showed two
425 populations of mono-peaks characterized by different T_{max} . By merging all the data, two peaks
426 or a plateau appear for the mean curve of the lipid-based and the amorphous formulation,
427 but are probably of different origin. Figure 7 shows the input rate of CBD absorption in
428 function of the animal and of the formulation (amorphous or lipid-based). It is clear that the
429 amorphous formulation presents a profile with at least two early peaks of absorption before 5
430 h, followed by a third smaller one, for all animal. The two first peaks occur therefore
431 independently of any meals administration as the animals were still fasted until the time point
432 6h. The third peak is less surprising, since it is linked to the first meal following administration
433 of the formulation. As the dissolution process from the amorphous formulation is not
434 characterized with successive release mechanisms, the successive phases of *in vivo*
435 absorption may indicate reabsorption and thus an EHC.

Amorphous

Lipid-based

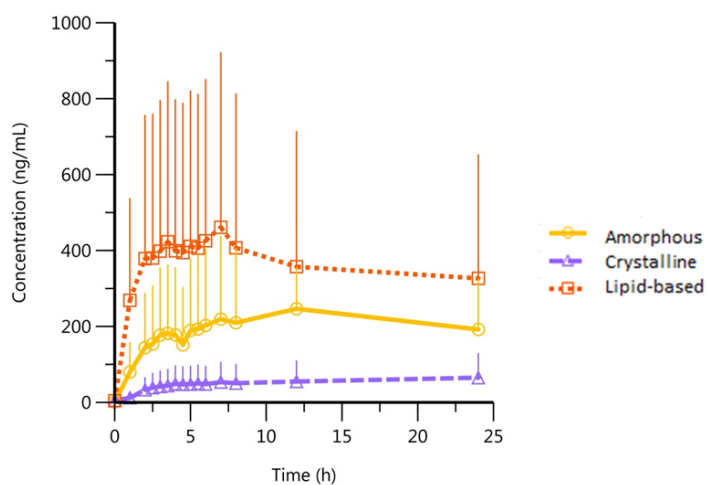


436
437

Figure 7 – Input rate of CBD absorption depending on animal and formulation

438 Considering the lipid-based formulation, if the later peak (corresponding to the third of
439 amorphous form and linked to the 6h post-dose meal) is also present among all animals, the
440 two first peaks are not always present. EHC may not systematically occur with the lipid-
441 based formulation and the apparent EHC would be rather due to the superimposition of early
442 population (T_{max} of 1 hour for P2, P5 and P6) and late population (T_{max} of 3 – 3.5 hours for P1
443 and P3)

444 As 7 – COOH – CBD was simultaneously quantified, the hepatic first pass degradation and
445 metabolization could be estimated. Figure 8 presents the mean profiles of 7 – COOH – CBD,
446 product of CBD metabolization, depending on the CBD formulation. This metabolization
447 occurs to provide more hydrophilic compound in order to accelerate the elimination of the
448 drug from the body. This secondary metabolite is inactive and follows the oxidation of the first
449 and active metabolite 7 – OH – CBD. These oxidations are described to mainly occur in the
450 liver by cytochromes enzymes and may thus partially represent the first-pass. However,
451 intravenous data showed that this first-pass is not on itself responsible of the early production
452 of oxidized metabolite. The formation of the carboxylate metabolite is thus due by a
453 combination of first-pass and systemic metabolization. Some lipid formulations are used to
454 overcome the first-pass metabolization. Authors have shown for example that the
455 administration of fatty acid (especially C16 and C18) in combination with lipophilic drugs,
456 which are prone to the first-pass effect, favor the formation of chylomicrons and the lymphatic
457 absorption (Franco et al., 2020). This lymphatic absorption allows to by-pass the liver first-
458 pass and so increases the bioavailability.



459

460

Figure 8 - 7 - COOH - CBD mean curves (\pm SD) after administration of an equivalent of 2.5 mg of CBD/kg (n=5)

461 Actually, the results were not expected since it was postulated that Gelucire protected CBD
462 to liver degradation by favoring the lymphatic transport. However, the AUC_{last} ratio
463 metabolite/CBD is much higher with the lipid-based formulation (95.33) than with the
464 amorphous formulation (33.37). The ratio obtained with the lipid formulation is quite similar
465 than the pure and crystalline CBD (93.87). The phenomenon explaining why the amorphous
466 form of CBD provided higher bioavailability and less hepatic degradation remains unclear
467 and precise investigations have to be conducted. It seems however intuitive that the
468 mesoporous silica amorphous loaded CBD lead to a tank that promotes supersaturation of
469 CBD within intestinal fluids. This supersaturated concentration increases the gradient and
470 accelerates the absorption rate. The hepatic enzymes are therefore more susceptible to be
471 saturated, promoting the passage of non-metabolized CBD in the bloodstream, translated by
472 a high AUC and low CBD/metabolite ratio and could explain higher variability as linked with
473 hepatic status and supersaturated state. In addition, it has been shown that CBD suffer from a
474 rapid systemic degradation when intravenously administrated. Since CBD metabolism is a
475 combination of hepatic and systemic degradation, the presence of lipids in the lipid-based
476 formulation involved in the lymphatic passage has only a limited impact on protection against
477 degradation. All of these differences may lead to the higher CBD bioavailability observed with
478 the amorphous formulation in comparison with the lipid-based formulation. Thanks to an
479 enterohepatic cycle and a reduced metabolization, the amorphous formulation allows
480 increasing the AUC_{last} of CBD, whose absorption seems to however depend on the presence
481 of digestive fluids and may lead to high variability. The lipid-based formulation, on the other
482 hand, offers the advantage of more reproducible bioavailability and less dependence on
483 digestive capacity, although it is smaller due to the absence of systematic enterohepatic
484 cycle and greater metabolism. While both the amorphous and lipid-based strategies are
485 interesting, the lipid-based formulation could be of greatest interest from a marketing
486 perspective, due to its definite increase in bioavailability, but also its lower variability when
487 administered to fasting individuals. This kind of formulation therefore reduces the food effects
488 (O'Shea et al., 2015), enabling better control of plasma concentrations and hence
489 therapeutic effects. What's more, the lipid-based formulation is very simple to produce and
490 requires no special equipment, making it easy to scale-up.

491 **Conclusion**

492 A CBD amorphous and CBD lipid-based formulations were tested and compared with
493 crystalline CBD in *in vitro* and *in vivo* conditions. Both optimized formulations allowed a
494 complete release of CBD within a maximum of 180 minutes in FaSSIF medium as the lipid-
495 based one slower the release due to more complex solubilization process. Both formulations

496 increased the bioavailability of CBD by 10.9-fold and 6.8-fold for the amorphous and lipid
497 formulations, respectively. A high inter piglet variability has been highlighted as well as a
498 potential enterohepatic cycle mainly for the amorphous formulation. The simultaneous
499 quantification of the metabolite 7 - COOH - CBD shows a higher metabolism from the
500 lipid-based formulation than from the amorphous one, demonstrating that the lipid strategy
501 was not advantageous to avoid the first pass effect. Besides, it has been shown that the lipid-
502 based formulation allows reducing the absorption variability.

503

504 **Supplementary materials**

505 **Table S1 - Mean of pharmacokinetic parameters (\pm SD) obtained from individual curves, including P4 (CBD dose 2.5**
506 **mg/kg; n=6)**

	Amorphous	Lipid-based	Crystalline
AUC _{last} (ng*h*mL ⁻¹)	126.07 \pm 79.00	81.34 \pm 46.25	30.09 \pm 42.02
C _{max} (ng/mL)	31.89 \pm 28.23	17.99 \pm 12.80	6.71 \pm 10.83
T _{max} (h)	5.4 \pm 3.54	2.0 \pm 1.14	6.5 \pm 8.61

507

508

509 **Acknowledgments**

510 This work was supported by FEDER funds (SOLPHARE project, [884148-329407](#)) and Fonds
511 Léon Frédéricq for the support in project 2021-2022-12.

512

513 **References**

514 Bergamaschi, M.M., Queiroz, R.H.C., Chagas, M.H.N., De Oliveira, D.C.G., De Martinis,
515 B.S., Kapczinski, F., Quevedo, J., Roesler, R., Schröder, N., Nardi, A.E., Martín-Santos,
516 R., Hallak, J.E.C., Zuardi, A.W., Crippa, J.A.S., 2011. Cannabidiol reduces the anxiety
517 induced by simulated public speaking in treatment-naïve social phobia patients.
518 *Neuropsychopharmacology* 36, 1219–1226. <https://doi.org/10.1038/npp.2011.6>

519 Bukara, K., Schueller, L., Rosier, J., Martens, M.A., Daems, T., Verheyden, L., Eelen, S.,
520 Van Speybroeck, M., Libanati, C., Martens, J.A., Van Den Mooter, G., Frérart, F.,

521 Jolling, K., De Gieter, M., Bugarski, B., Kiekens, F., 2016. Ordered mesoporous silica to
522 enhance the bioavailability of poorly water-soluble drugs: Proof of concept in man. *Eur.*
523 *J. Pharm. Biopharm.* 108, 220–225. <https://doi.org/10.1016/j.ejpb.2016.08.020>

524 Cardot, J.M., Davit, B.M., 2012. In vitro-in vivo correlations: Tricks and traps. *AAPS J.* 14,
525 491–499. <https://doi.org/10.1208/s12248-012-9359-0>

526 Corsaro, C., Neri, G., Mezzasalma, A.M., Fazio, E., 2021. Weibull modeling of controlled
527 drug release from Ag-PMA nanosystems. *Polymers (Basel)*. 13.
528 <https://doi.org/10.3390/polym13172897>

529 De Prá, M.A.A., Vardanega, R., Loss, C.G., 2021. Lipid-based formulations to increase
530 cannabidiol bioavailability: In vitro digestion tests, pre-clinical assessment and clinical
531 trial. *Int. J. Pharm.* 609. <https://doi.org/10.1016/j.ijpharm.2021.121159>

532 Feeney, O.M., Crum, M.F., McEvoy, C.L., Trevaskis, N.L., Williams, H.D., Pouton, C.W.,
533 Charman, W.N., Bergström, C.A.S., Porter, C.J.H., 2016. 50 years of oral lipid-based
534 formulations: Provenance, progress and future perspectives. *Adv. Drug Deliv. Rev.* 101,
535 167–194. <https://doi.org/10.1016/j.addr.2016.04.007>

536 Fonseca, B.M., Rebelo, I., 2022. Cannabis and Cannabinoids in Reproduction and Fertility:
537 Where We Stand. *Reprod. Sci.* 29, 2429–2439. [https://doi.org/10.1007/s43032-021-](https://doi.org/10.1007/s43032-021-00588-1)
538 [00588-1](https://doi.org/10.1007/s43032-021-00588-1)

539 Franco, V., Gershkovich, P., Perucca, E., Bialer, M., 2020. The Interplay Between Liver First-
540 Pass Effect and Lymphatic Absorption of Cannabidiol and Its Implications for
541 Cannabidiol Oral Formulations. *Clin. Pharmacokinet.* 59, 1493–1500.
542 <https://doi.org/10.1007/s40262-020-00931-w>

543 Grifoni, L., Vanti, G., Donato, R., Sacco, C., Bilia, A.R., 2022. Promising Nanocarriers to
544 Enhance Solubility and Bioavailability of Cannabidiol for a Plethora of Therapeutic
545 Opportunities. *Molecules* 27. <https://doi.org/10.3390/molecules27186070>

546 Heider, C.G., Itenberg, S.A., Rao, J., Ma, H., Wu, X., 2022. Mechanisms of Cannabidiol
547 (CBD) in Cancer Treatment: A Review. *Biology (Basel)*. 11.
548 <https://doi.org/10.3390/biology11060817>

549 Henze, L.J., Koehl, N.J., O'Shea, J.P., Kostewicz, E.S., Holm, R., Griffin, B.T., 2019. The pig
550 as a preclinical model for predicting oral bioavailability and in vivo performance of
551 pharmaceutical oral dosage forms: a PEARRL review. *J. Pharm. Pharmacol.* 71, 581–

552 602. <https://doi.org/10.1111/jphp.12912>

553 Jennotte, O., Koch, N., Lechanteur, A., Evrard, B., 2022. Development of amorphous solid
554 dispersions of cannabidiol: Influence of the carrier, the hot-melt extrusion parameters
555 and the use of a crystallization inhibitor. *J. Drug Deliv. Sci. Technol.* 71, 103372.
556 <https://doi.org/10.1016/j.jddst.2022.103372>

557 Koch, N., Jennotte O., Ziemons E., Boussard G., Lechanteur A., E.B., 2022. Influence of API
558 physico-chemical properties on amorphization capacity of several mesoporous silica
559 loading methods. *Int. J. Pharm.* 613, 121372.
560 <https://doi.org/https://doi.org/10.1016/j.ijpharm.2021.121372>

561 Koch, N., Jennotte, O., Gasparrini, Y., Vandenbroucke, F., Lechanteur, A., Evrard, B., 2020.
562 Cannabidiol aqueous solubility enhancement: Comparison of three amorphous
563 formulations strategies using different type of polymers. *Int. J. Pharm.* 589.
564 <https://doi.org/10.1016/j.ijpharm.2020.119812>

565 Koch, N., Jennotte, O., Lechanteur, A., Deville, M., Charlier, C., Cardot, J., Chiap, P., Evrard,
566 B., 2024. An Intravenous Pharmacokinetic Study of Cannabidiol Solutions in Piglets
567 through the Application of a Validated Ultra-High-Pressure Liquid Chromatography
568 Coupled to Tandem Mass Spectrometry Method for the Simultaneous Quantification of
569 CBD and Its Carboxylated Metabolite in Plasma. *Pharmaceutics* 16(1).
570 <https://doi.org/https://doi.org/10.3390/pharmaceutics16010140>

571 Koch, N., Jennotte, O., Toussaint, C., Lechanteur, A., Evrard, B., 2023. Production
572 challenges of tablets containing lipid excipients: Case study using cannabidiol as drug
573 model. *Int. J. Pharm.* 633. <https://doi.org/10.1016/j.ijpharm.2023.122639>

574 McCarthy, C.A., Faisal, W., O'Shea, J.P., Murphy, C., Ahern, R.J., Ryan, K.B., Griffin, B.T.,
575 Crean, A.M., 2017. In vitro dissolution models for the prediction of in vivo performance
576 of an oral mesoporous silica formulation. *J. Control. Release* 250, 86–95.
577 <https://doi.org/10.1016/j.jconrel.2016.12.043>

578 Mellaerts, R., Mols, R., Jammaer, J.A.G., Aerts, C.A., Annaert, P., Van Humbeeck, J., Van
579 den Mooter, G., Augustijns, P., Martens, J.A., 2008. Increasing the oral bioavailability of
580 the poorly water soluble drug itraconazole with ordered mesoporous silica. *Eur. J.*
581 *Pharm. Biopharm.* 69, 223–230. <https://doi.org/10.1016/j.ejpb.2007.11.006>

582 Millar, S.A., Stone, N.L., Bellman, Z.D., Yates, A.S., England, T.J., O'Sullivan, S.E., 2019. A
583 systematic review of cannabidiol dosing in clinical populations. *Br. J. Clin. Pharmacol.*

584 85, 1888–1900. <https://doi.org/10.1111/bcp.14038>

585 Millar, S.A., Stone, N.L., Yates, A.S., O’Sullivan, S.E., 2018. A systematic review on the
586 pharmacokinetics of cannabidiol in humans. *Front. Pharmacol.* 9.
587 <https://doi.org/10.3389/fphar.2018.01365>

588 Noblet, J., Gilbert, H., Jaguelin-Peyraud, Y., Lebrun, T., 2013. Evidence of genetic variability
589 for digestive efficiency in the growing pig fed a fibrous diet. *Animal* 7, 1259–1264.
590 <https://doi.org/10.1017/S1751731113000463>

591 O’Shea, J.P., Faisal, W., Ruane-O’Hora, T., Devine, K.J., Kostewicz, E.S., O’Driscoll, C.M.,
592 Griffin, B.T., 2015. Lipidic dispersion to reduce food dependent oral bioavailability of
593 fenofibrate: In vitro, in vivo and in silico assessments. *Eur. J. Pharm. Biopharm.* 96,
594 207–216. <https://doi.org/10.1016/j.ejpb.2015.07.014>

595 O’Shea, J.P., Nagarsekar, K., Wieber, A., Witt, V., Herbert, E., O’Driscoll, C.M., Saal, C.,
596 Lubda, D., Griffin, B.T., Dressman, J.B., 2017. Mesoporous silica-based dosage forms
597 improve bioavailability of poorly soluble drugs in pigs: case example fenofibrate. *J.*
598 *Pharm. Pharmacol.* 69, 1284–1292. <https://doi.org/10.1111/jphp.12767>

599 Papadopoulou, V., Kosmidis, K., Vlachou, M., Macheras, P., 2006. On the use of the Weibull
600 function for the discernment of drug release mechanisms. *Int. J. Pharm.* 309, 44–50.
601 <https://doi.org/10.1016/j.ijpharm.2005.10.044>

602 Perlstein, H., Bavli, Y., Turovsky, T., Rubinstein, A., Danino, D., Stepensky, D., Barenholz,
603 Y., 2014. Beta-casein nanocarriers of celecoxib for improved oral bioavailability. *Eur. J.*
604 *Nanomedicine* 6, 217–226. <https://doi.org/10.1515/ejnm-2014-0025>

605 Perucca, E., Bialer, M., 2020. Critical Aspects Affecting Cannabidiol Oral Bioavailability and
606 Metabolic Elimination, and Related Clinical Implications. *CNS Drugs* 34, 795–800.
607 <https://doi.org/10.1007/s40263-020-00741-5>

608 Rapin, L., Gamaoun, R., El Hage, C., Arboleda, M.F., Prosk, E., 2021. Cannabidiol use and
609 effectiveness: real-world evidence from a Canadian medical cannabis clinic. *J.*
610 *Cannabis Res.* 3. <https://doi.org/10.1186/s42238-021-00078-w>

611 Riikonen, J., Correia, A., Kovalainen, M., Näkki, S., Lehtonen, M., Leppänen, J., Rantanen,
612 J., Xu, W., Araújo, F., Hirvonen, J., Järvinen, K., Santos, H.A., Lehto, V.P., 2015.
613 Systematic in vitro and in vivo study on porous silicon to improve the oral bioavailability
614 of celecoxib. *Biomaterials* 52, 44–55. <https://doi.org/10.1016/j.biomaterials.2015.02.014>

- 615 Tomic, I., Mueller-Zsigmondy, M., Vidis-Millward, A., Cardot, J.M., 2018. In vivo release of
616 peptide-loaded PLGA microspheres assessed through deconvolution coupled with
617 mechanistic approach. *Eur. J. Pharm. Biopharm.* 125, 21–27.
618 <https://doi.org/10.1016/j.ejpb.2017.12.007>
- 619 Trevaskis, N.L., Charman, W.N., Porter, C.J.H., 2008. Lipid-based delivery systems and
620 intestinal lymphatic drug transport: A mechanistic update. *Adv. Drug Deliv. Rev.* 60,
621 702–716. <https://doi.org/10.1016/j.addr.2007.09.007>
- 622 Yáñez, J.A., Wang, S.W.J., Knemeyer, I.W., Wirth, M.A., Alton, K.B., 2011. Intestinal
623 lymphatic transport for drug delivery. *Adv. Drug Deliv. Rev.* 63, 923–942.
624 <https://doi.org/10.1016/j.addr.2011.05.019>
- 625 Zhang, Z., Quan, G., Wu, Q., Zhou, C., Li, F., Bai, X., Li, G., Pan, X., Wu, C., 2015. Loading
626 amorphous Asarone in mesoporous silica SBA-15 through supercritical carbon dioxide
627 technology to enhance dissolution and bioavailability. *Eur. J. Pharm. Biopharm.* 92, 28–
628 31. <https://doi.org/10.1016/j.ejpb.2015.02.018>

629